# Evaluation of Hemispheric Dominance for Language Using Functional MRI: A Comparison With Positron Emission Tomography

**Jinhu Xiong,**[1*] **Shobini Rao,**[2] **Jia-Hong Gao,**[1] **Marty Woldorff,**[1] **and Peter T. Fox**[1]

[1]*Research Imaging Center, University of Texas Health Science Center, San Antonio, Texas 78284-6240*
[2]*Department of Clinical Psychology, National Institute of Mental Health and Neurosciences, Bangalore, India*

◆━━━━━━━━━━━━━━━━━━━━━━━━━━━━━━━━━━━━━━◆

**Abstract:** The utility of a conventional (i.e., nonecho-planar) functional magnetic resonance imaging (fMRI) technique to determine hemispheric dominance for language was assessed using a semantic generation task in which subjects were presented with a series of nouns and generated aloud a verb for each one. A direct comparison of the fMRI results with positron emission tomography (PET), acquired from the same subjects, was also performed. When analyzed by group averaging, the results of this work were in concordance with those of previous PET studies, showing a left hemispheric dominance for language. Analyzed on an individual basis, 7 out of 9 subjects were left-hemisphere dominant and 2 subjects were right-hemisphere dominant; this applied with both PET and fMRI methods. The direct comparison between PET and fMRI further demonstrated that fMRI can replicate PET findings. Of the total activation foci detected by PET, 92% were observed by fMRI. On the other hand, fMRI reported 64% more activations than did PET. This may reflect differences in procedure, spatial resolution, sensitivity, and the underlying physiological mechanism between PET and fMRI. This study suggests that the fMRI technique, even using conventional MRI scanners, could be clinically useful in evaluating hemispheric dominance for language on an individual subject-by-subject basis. *Hum. Brain Mapping 6:42–58, 1998.*    © 1998 Wiley-Liss, Inc.

**Key words:** fMRI; PET; language; cognition; hemispheric dominance; lateralization

◆━━━━━━━━━━━━━━━━━━━━━━━━━━━━━━━━━━━━━━◆

## INTRODUCTION

Functional magnetic resonance imaging (fMRI) has become a popular approach for mapping human brain activation. Currently, this technique typically relies on blood-oxygen-level-dependent (BOLD) contrast by de-

tecting local hyperoxia [Fox et al., 1988] as evidenced by a reduction in the paramagnetic effect of hemoglobin [Kwong et al., 1992; Ogawa et al., 1992; Bandettini et al., 1992; Schneider et al., 1993; Constable et al., 1993; Schad et al., 1994]. Since the first report of using the BOLD technique to map the primary visual and motor cortex by Kwong et al. [1992], an increasing number of studies have been documented for mapping neural processes of perception [Ogawa et al., 1992; Menon et al., 1992; Schneider et al., 1993], action [Bandettini et al., 1992, 1993a,b; Kim et al., 1993; Rao et al., 1993], and cognition [Cohen et al., 1994; McCarthy et al., 1993; Shaywitz et al., 1995a,b] of the human brain.

In addition to studies of normal healthy volunteers, the fMRI technique also has great clinical potential for the preoperative identification of cerebral dominance for language and memory to prevent a postoperative neurologic deficit (such as loss of language). Traditionally, the most commonly performed preoperative test for cerebral dominance has been the Wada test [Wada, 1949; Wada and Rasmussen, 1960], which uses arterial injection of anesthetic to one side of the brain of a time while testing speech. This test is highly invasive, however, and suffers from very low resolution (i.e., left vs. right hemisphere only), high cost, and high risk. A new procedure, using positron emission tomography (PET) to assess language dominance with a visual word task, was reported by Pardo and Fox [1993]. These authors reported this approach to be at least as accurate as the Wada test for determining hemispheric dominance, but with substantially lower risk and considerably higher spatial resolution. This technique, however, has its own limitations, such as radioactive exposure to the patient, only moderate spatial resolution (5–20 mm), and availability in relatively few centers around the world. Functional MRI, on the other hand, is completely noninvasive, has higher spatial resolution (1–4 mm), and is more widely available. Thus, it offers the possibility of preoperative identification of hemisphere dominance for language.

Before being considered for clinical possibilities, however, it would be useful to directly compare language activations and lateralization assessed by fMRI to those assessed by PET. Up to now, studies of the ability of fMRI to assess the hemispheric dominance for language and memory have produced mixed results. For example, in normal, healthy right-handed volunteers, bilateral activations in the frontal lobes have been observed for language using fMRI [Shaywitz et al., 1995a,b; McCarthy et al., 1993], providing no evidence for lateralization [Shaywitz et al., 1995a]. Similar findings were reported regarding nonspatial working memory studies, again revealing no significant effect of hemisphere [Cohen et al., 1993, 1994]. These findings are in direct conflict with the results of PET experiments for normal, healthy right-handed volunteers, which demonstrated left-hemispheric dominance for both language [Petersen et al., 1988, 1989; Wise et al., 1991] and nonspatial working memory [Sergent et al., 1992; Paulesu et al., 1993, 1995; Shallice et al., 1994].

The fMRI results for epileptic patients, however, appear to contradict those for normal volunteers. Preliminary studies in preoperative mapping for epileptic patients suggest that the hemispheric dominance for language could be determined using fMRI [Hertz-Pannier et al., 1994; Binder et al., 1995; Desmond et al., 1995]. As with PET [Pardo and Fox, 1993], the laterality of language dominance in these patients as assessed by fMRI has generally been found to be quite consistent with that determined by the Wada test.

In short, the results of the fMRI normal-volunteer studies contradict those for the PET normal-volunteer studies, PET patient studies, and fMRI patient studies. The reasons behind these conflicting results are of great interest and are not yet clear. Thus, it is extremely valuable to assess the ability of fMRI in determining the hemispheric dominance for language in normal healthy volunteers, and to compare fMRI with PET for assessing to what extent the fMRI BOLD technique correlates with the regional cerebral blood flow (rCBF) change detected with PET.

In this paper, we focus on the assessment of hemispheric dominance for language using a semantic (verb) generation task. Two studies were performed: 1) a PET/fMRI study, and 2) an fMRI-only study. A direct comparison of PET and fMRI brain activation data, acquired from the same subjects, was performed to determine to what extent the fMRI findings correlated with the PET study. For the PET/fMRI comparison, the PET data were acquired over the entire brain volume (15 slices) in each individual subject. An individual subject-by-subject analysis (no intersubject averaging) was used to locate the activation foci associated with the verb generation paradigm. A single-slice sampling was used for fMRI, with the slice location determined by the peak activation detected in the frontal regions by PET for each volunteer. For the fMRI-only study, the fMRI slice was positioned as a standardized location, and not individually optimized. The anatomical plane selected was determined from the PET/fMRI study as that most likely to demonstrate hemispheric lateralization. Thus, the PET/fMRI study sought 1) to determine the degree of correlation between these two imaging methods, and 2) to further confirm the ability of both methods to evaluate hemispheric dominance for language. The fMRI-only study sought to determine the practical utility of a single-slice, conventional (nonechoplanar) fMRI for assessing hemispheric dominance for language.

## MATERIALS AND METHODS

Two studies were performed: 1) a PET/fMRI study, and 2) an fMRI-only study. The PET experiment was performed and analyzed first. The locations of activations from PET were used to guide fMRI slice selection for both fMRI studies. The guidance strategy, however, differed between the two studies. In the PET/fMRI

study, slice guidance was optimized for each person. For the fMRI-only study, slice selection was guided by the group-mean PET response.

## Subjects

Eighteen normal healthy volunteers, ranging in age from 21–50 years, participated in this study. All subjects were native English speakers. Subjects are reported as two groups: group 1, PET/fMRI, and group 2, fMRI-only. Group 1 consisted of 5 male and 4 female subjects, all right-handed. All 9 subjects were scanned with PET; 6 of the 9 subjects subsequently underwent the fMRI activation study, with 3 subjects unable to return for the fMRI study. The PET experiments were always performed first. The fMRI experiments were performed at least 6 months later to minimize the familiarity effects associated with the task material [Raichle et al., 1994]. Group 2 (fMRI-only) consisted of 1 left-handed and 8 right-handed volunteers (5 males and 4 females).

## Subject preparation

PET and MRI scans were acquired with the subject supine and with the head supported in a foam-padded, hemicylindrical head holder. Head position in PET was adjusted with the aid of laser alignment beams. The subject's head was immobilized within a tightly fitting, thermally molded, plastic facial mask [Fox et al., 1985]. The mask extended from hairline to chin. For the fMRI study, the portion of the mask that touched the subject's chin was cut out to make it easier for the subject to speak aloud without head motion.

## Task paradigms

The semantic (verb) generation task was used to assess hemispheric lateralization for language. A list of 502 concrete nouns was chosen from the list of Paivio et al. [1968] and from the lists of frequent words of Francis and Kucera [1982]. Word length ranged from 3–7 letters. For the PET study, three lists of 90 nouns each were constructed to be used during scanning. Two lists of 20 nouns each served as a practice list. Words did not repeat either within or between lists. For the fMRI study, the same words were reconstructed to seven lists of 70 words each. A list of 12 words formed the practice list. Again, words did not repeat either within or between lists.

Two behavioral conditions are reported: control and activation. During the control state, the subject was asked to fixate on a cross hair presented in the center of a screen. During the activation state, the nouns were presented to the subject, who was instructed to generate aloud an associated verb for each noun. For the PET study, words were displayed above the cross hair in the center of a video monitor and subtended approximately 1.2° vertically and 5.7° horizontally. For the fMRI study, words were also displayed above the cross hair and were projected into the bore of the scanner and onto a back projection screen about 5 inches above the subject's eyes through a Sharp LCD projector (XV-H30U, Sharp Co., Japan), a focus lens, and a reflection mirror. The subject viewed the stimulus by looking up and into a tilted mirror. The subtended angle of the words in fMRI was similar to that in PET. For both PET and fMRI, words were presented for a duration of 150 msec at the rate of 1/sec. Subjects were familiarized with the task by exposure to the practice list before entering the scanner.

## Data acquisition

### PET scans

PET data were acquired with a GE/Scanditronix 4096 camera. This camera simultaneously acquires 15 parallel slices with a center-center interslice distance of 6.5 mm and a transaxial field of view of 10.5 cm. Images were reconstructed at an in-plane resolution of 8-mm full width at half maximum (FWHM) and an axial resolution of 6.5 mm FWHM. Before emission scanning, a 15-slice tomographic transmission image (68 Ge/68 Ga) system was obtained for calculating regional attenuation coefficients [Fox et al., 1985]. Water labeled with oxygen-15 ($H_2^{15}O$, half-life 123 sec) was used as a blood-flow tracer. Between 70–75 mCi of $H_2^{15}O$ in 5–10 cc of sterile saline were delivered as an intravenous bolus. Data acquisition began as the tracer bolus arrived in the brain (15–20 sec after tracer injection) and continued for 40 sec. For the activation condition, stimulus presentation and task began at the same time as tracer injection. Each subject underwent a series of nine scans of brain blood flow (three scans each of three conditions). Two of the three conditions are reported here. A 10–15-min interscan interval was sufficient for isotopic decay (five half-lives) and to reestablish resting levels of brain blood flow before the subsequent scan.

### Anatomical MRI scans

MRI experiments were performed on an Elscint Gyrex 2-T whole-body MRI scanner (Elscint Ltd., Haifa, Israel) operating at 1.9 T. For every volunteer

participating in the PET study, a three-dimensional (3D) T1-weighted anatomical image was acquired for the entire brain, with a voxel size of $1.0 \times 1.0 \times 1.2$ mm for PET-MRI coregistration. Before the fMRI study, a set of three T1-weighted images (coronal, transverse, and sagittal) was acquired to locate and orient the fMRI slice. Multiple-slice T1-weighted spin-echo images were first obtained in the coronal plane to identify the interhemispheric fissure. A transverse T1-weighted image was then acquired in an orientation perpendicular to the interhemispheric fissure. Consequently, a sagittal T1-weighted image was positioned along the interhemispheric fissure defined by the transverse image, allowing localization of the anterior commissure and posterior commissure. Finally, the fMRI slice was oriented in a transverse plane parallel to the AC-PC line. This procedure guaranteed that the functional slice was parallel to the AC-PC line and, at the same time, perpendicular to the interhemispheric fissure. At the end of fMRI data collection, a T1-weighted anatomical image in the same position was acquired to facilitate precisely determining the structures corresponding to the functional activation foci.

### fMRI planes

All fMRI data were acquired in a transverse plane parallel to the AC-PC line and perpendicular to the interhemispheric fissure, as defined with the procedure described above. For PET/fMRI comparison (group 1 subjects), slice position was determined for each individual subject and was selected to pass through the plane of peak activation in the frontal lobes in the PET data. The slice position varied from subject to subject because location of the peak activation varied across subjects. For the fMRI-only study (group 2 subjects), slice position was guided by the group mean PET data, which indicated the plane of maximum laterality as being 4 mm above the AC-PC line. This plane was then selected for group 2 subjects.

### fMRI scans

For the fMRI study, a T2*-weighted gradient-echo pulse sequence was used with a TR/TE/flip-angle of 60 msec/40 msec/20°. The slice thickness was 10 mm for group 1 subjects and either 6 or 10 mm for group 2 subjects; the field of view was $256 \times 256$ mm²; and the acquisition matrix was $128 \times 256$. Typically, 8 sec were required to acquire one imaging data set. Seven resting-stimulated (i.e., control-activation) cycles with eight images per state per cycle were acquired for each section. The raw data were zero-filled to a matrix of

$256 \times 256$ before reconstruction. Data analysis software was programmed in Matlab (MathWorks Inc., Natick, MA).

### Data analysis

#### PET data analysis

The PET and the 3D MRI T1-weighted images were spatially normalized [Fox et al., 1985; Lancaster et al., 1995] into registration with the Talairach brain atlas [Talairach and Tournoux, 1988]. Using a nine-parameter fit and interactive denotation of the AC-PC line, the images were resliced into 60 slices using trilinear interpolation, with image matrix size $60 \times 128 \times 128$, a slice thickness of 2 mm, and each voxel $2 \times 2 \times 2$ mm³. PET images were value-normalized to a whole brain of 50 ml/100 g/min. Each control scan was subtracted independently from the verb generation scan nearest in time, and a mean subtraction image was obtained for each individual subject. Subsequent calculations were performed on these mean subtraction images.

The PET subtraction images were further analyzed to define the significant activations in order to provide guidance for the fMRI slice selection. The distribution of the magnitudes of local blood-flow change was tested for the existence of significant outliers using an omnibus gamma-2 test [Fox et al., 1988]. The presence of significant outliers indicated by the gamma-2 test indicated significant activation. Then, identification of these outliers (i.e., pixels with significant increases of blood flow) was accomplished through a local extrema search. A search cube of 125 mm³ was applied on each pixel. The pixel with the highest value within this cube was designated as the maxima point. The x-, y-, and z-coordinates of the maxima points were calculated in the Talairach atlas coordinate [Talairach and Tournoux, 1988]. The change in intensity of blood flow compared to mean quantity of blood flow in the image was calculated for each maxima point. The change in intensity of blood flow in each maxima point was also given a z-score with respect to the standard deviation of the population of all brain voxels in the subtraction image. The extent of activation was determined through cluster analysis [Mintun et al., 1989], using a cluster-size search cube of 125 mm³ applied around each maxima point. Those points that were within this cube and whose z-score exceeded a significance of $P < 0.01$ were included in the cluster. This analysis was used to guide the fMRI slice selection.

To enable direct PET/fMRI comparison, the PET images were linearly interpolated to an image matrix size of $256 \times 256$ and were resliced with a slice

thickness of 10 mm, to match the fMRI slice. A z-score image was created for each subject. The slice corresponding to the location of the fMRI slice was further analyzed using the same procedure (clustered-pixels analysis procedure) for fMRI data analysis, as described in the following section. This data analysis strategy assesses statistical significance based on both intensity threshold (t), and cluster-size threshold (K), and has higher statistical power than the conventional intensity-only threshold technique [Xiong et al., 1995]. The optimal intensity threshold and extent threshold were determined to be t = 3.7 and K = 14 for a significance level of 0.05 with a searched brain area of 16,000 pixels and a spatial resolution of 8 mm FWHM.

### fMRI data analysis

For PET/fMRI comparison, fMRI data were also spatially normalized into registration with the Talairach brain atlas [Talairach and Tournoux, 1988]. Motion correction was performed as necessary by using the automated registration algorithm published by Woods et al. [1993]. The fMRI data were then analyzed using the clustered-pixels analysis procedure developed by Xiong et al. [1995]. As required for this procedure, a statistical parametric image (SPI) was first created using a pixel-by-pixel group t-test. The SPI was then thresholded using an intensity threshold of t = 2.5, and the suprathreshold pixels were then searched. The clusters of pixels were identified with a four-connectivity algorithm (pixels that share a common edge are connected). In addition to the t-value threshold, the spatial extent of brain activations was also taken into account in assessing the significance level. A spatial extent threshold (specified cluster size), K, which is a function of intensity threshold t (t = 2.5), significance $P$ ($P = 0.05$ in this study), area of the searched brain region (16,000 pixels used in this study), and FWHM of the spatial resolution of the SPI ($FWHM_t = 1.4$ pixels for this study), was determined to be five pixels [Xiong et al., 1995]. Only pixel clusters larger than or equal to this specified size K were considered to be a real fMRI signal; clusters with a size less than K were considered to be noise and were eliminated from the final functional image. The functional activation information was displayed in color scale and was superimposed onto the T1-weighted anatomic image in gray scale.

### Lateralization index (LI)

To quantify the asymmetry in functional activation, regions of interest (ROIs) were selected a priori based on the stereotactic coordinates of language processing centers as described by Petersen et al. [1988, 1989] and Wise et al. [1991]. These studies had shown that a verb generation task activated several brain regions, with strong laterality to the left hemisphere in normal healthy volunteers. These regions include the anterior inferior frontal cortex (Brodmann areas (BAs) 45–47), posterior inferior frontal cortex (BA 44), and posterior superior temporal cortex (BA 22). To determine to what extent a particular brain region is involved in a particular task, the intensity, spatial extent, and number of activations should be taken into account. For each of the significant activation foci, an intensity-weighted area of activation was calculated, which is defined here as the integral of intensity over that significantly activated region and which thus includes the combined effects of intensity and spatial extent for that area. These intensity-weighted volumes could then be combined to calculate the lateralization index (LI). The intensity-weighted volumes of the significant activations were calculated for BAs 44–47, and 22 for both left and right hemispheres. An LI was computed for each individual subject from these areas by the following equation [Binder et al., 1995; Desmond et al., 1995]:

$$LI = \frac{\sum_i s_{li} - \sum_i s_{ri}}{\sum_i s_{li} + \sum_i s_{ri}} = \sum_i s'_{li} - \sum_i s'_{ri} \qquad (1)$$

where $s_{li}$ and $s_{ri}$ denote the intensity-weighted areas of the activations in the ith left-side and right-side ROIs, respectively; $s'_{li} = s_{li}/(\Sigma_i s_{li} + \Sigma_i s_{ri})$ and $s'_{ri} = s_{ri}/(\Sigma_i s_{li} + \Sigma_i) s_{ri}$ are the normalized intensity-weighted areas of the activations in the ith left-side and right-side ROIs. The value of the LI can range from $-1-+1$. A negative value indicates right-hemispheric dominance; a positive value indicates left-hemispheric dominance; and a value near zero indicates no dominant hemisphere (or indeterminant). For purposes of the present study, we chose $|LI| < 0.1$ as the cutoff for indeterminant.

### RESULTS

#### PET-fMRI comparison

Figure 1 illustrates an average PET activation map for the group of 9 right-handed normal volunteers (group 1). As expected, significant activations were predominantly observed in the left inferior frontal gyrus (BAs 45–47), Broca's area (BA 44/6), and the left superior temporal gyrus (BA 22), providing strong
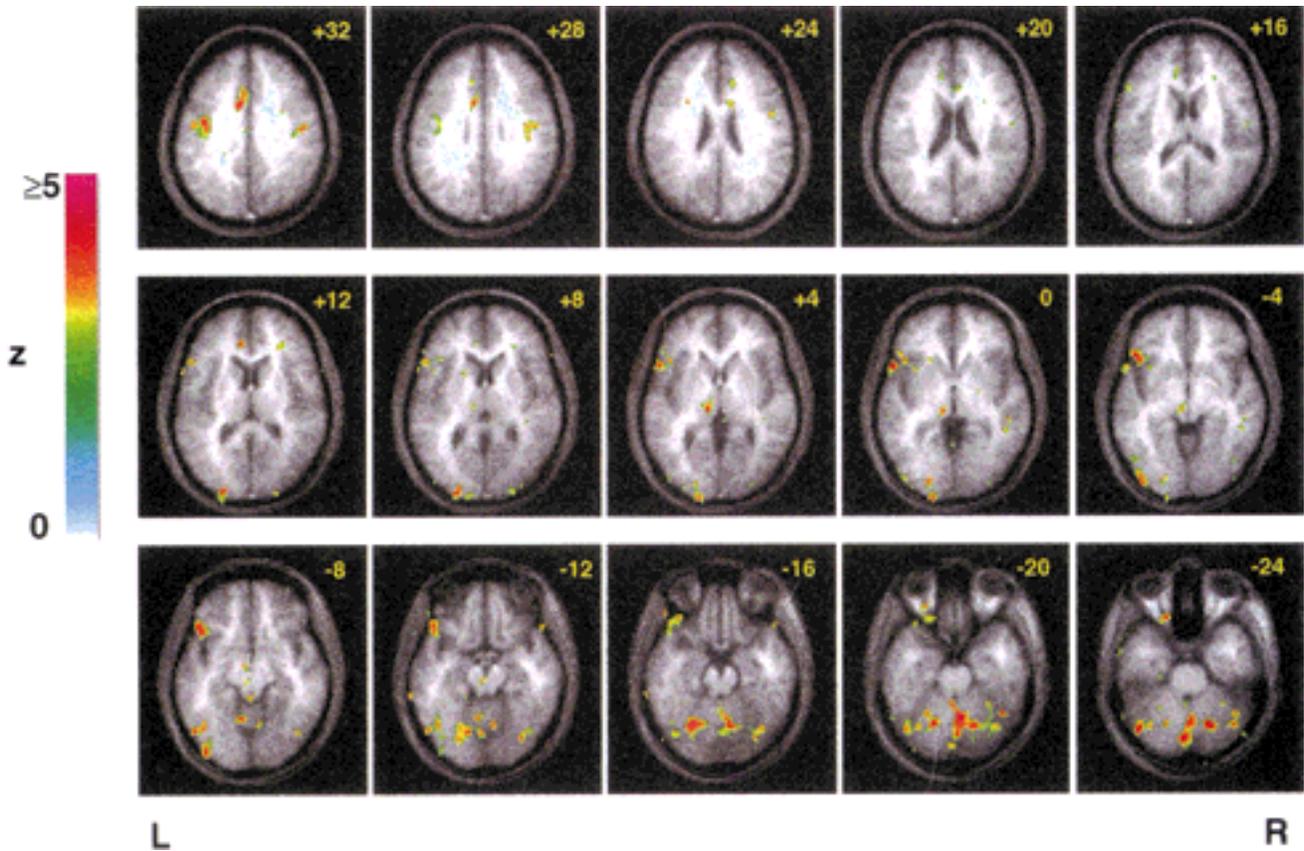
**Figure 1.**

Significant PET activations during verb generation task. Activation information has been transformed into stereotactic space, averaged across the 9 subjects in group 1, and overlaid on the spatially normalized, averaged anatomical T1-weighted MRI images. Color scale represents t value of each pixel. Numbers at upper right refer to distance of this slice in millimeters from AC-PC plane. R, right hemisphere; L, left hemisphere.

evidence for left-hemispheric dominance. Activation foci were also found in the cingulate gyrus (BAs 32 and 24), inferior temporal gyrus (BA 37), and the occipital gyri (BAs 18 and 19), with activations in the left hemisphere appearing to be stronger than in the right hemisphere. Additional activations were also seen in the basal ganglia, thalamus, insula, and cerebellum.

Although the group of subjects showed left-hemispheric dominance for language, this does not ensure that all subjects in the group are left-hemisphere dominant. The lateralization indices for individual subjects are summarized in Table I. The values of the lateralization index ranged from $-0.39$–$+1.00$, with a positive value indicating left-hemispheric dominance for language and a negative value indicating right-hemispheric dominance. The PET results showed that 7 out of 9 right-handed subjects exhibited left-hemispheric dominance, but 2 out of 9 (subjects 1.6 and 1.8, both females) exhibited right-hemispheric dominance. When restricted to the brain volume sampled by fMRI, both the fMRI results and the PET results for this limited brain volume were in agreement with the whole-brain PET results for 5 subjects. The LI value of PET (the limited brain volume) for another subject (subject 1.6) was close to zero and showed no lateralization effect. The fMRI result for this subject disagreed with the PET findings, in which the PET (whole brain) indicated right-hemispheric dominance but the fMRI indicated left-hemispheric dominance. The other 3 subjects of the 9 were unable to return for the fMRI study.

Table II summarizes the number of activations detected using PET and fMRI for individual subjects. For direct PET and fMRI comparison, only the PET activations located within the brain volume sampled by fMRI were reported. Table II indicates that 92% of the

TABLE I. PET and fMRI assessment of hemispheric dominance for language for right-handed normal volunteers*

| Subject | 1.1 | 1.2 | 1.3 | 1.4 | 1.5 | 1.6 | 1.7 | 1.8 | 1.9 |
|---|---|---|---|---|---|---|---|---|---|
| Gender | Male | Male | Female | Male | Male | Female | Female | Female | Male |
| Whole brain | | | | | | | | | |
| PET LI | 1.00 | 0.31 | 0.89 | 0.68 | 0.83 | −0.39 | 0.72 | −0.13 | 0.87 |
| Laterality | Left | Left | Left | Left | Left | Right | Left | Right | Left |
| Limited brain volume | | | | | | | | | |
| PET LI | 0.64 | 0.77 | 0.46 | 1.00 | 1.00 | −0.05 | | | |
| Laterality | Left | Left | Left | Left | Left | Indet. | | | |
| fMRI LI | 0.86 | 0.62 | 0.30 | 0.58 | 0.16 | 0.58 | | | |
| Laterality | Left | Left | Left | Left | Left | Left | | | |

\* LI, lateralization index computed using the intensity-weighted area of BAs 22 and 44–47. Limited brain volume, brain volume samples by fMRI. Indet., indeterminant. Laterality was classified as indeterminant if $|L\| < 0.1$.

PET activations were duplicated by fMRI. This demonstrated that fMRI is quite reliable in terms of replication of PET findings. On the other hand, fMRI detected 64% more activations than did PET. This may reflect differences in mechanism, procedure, spatial resolution, and/or sensitivity between PET and fMRI (for more details, refer to Discussion).

Detailed brain activation information during verb generation is shown for each subject in Tables III–VIII and described below. Again, only the PET activations located within the brain volume sampled by fMRI were reported.

### Subject 1.1 (Table III)

The PET experiment revealed activation foci in the left inferior frontal gyrus (BAs 44 and 45), the left superior temporal gyrus (BA 22), the right inferior frontal gyrus (BA 44), and the right caudate. All activations observed by PET were also observed by fMRI. Additionally, fMRI showed activations in the left caudate, the right superior temporal gyri (BA 22), and the bilateral middle occipital gyri (BAs 18 and 19). The significant activations for both PET and fMRI are shown in Figure 2.

### Subject 1.2 (Table IV)

PET and fMRI both found activations in the inferior frontal gyrus (BA 47), left superior temporal gyrus (BA 38), and left inferior temporal gyrus (BA 37), as well as the optic chiasm, left brain stem, and cerebellum. However, fMRI showed additional activations in the right inferior temporal gyrus (BA 37), left middle temporal gyrus (BA 21), and left parahippocampal gyrus.

### Subject 1.3 (Table V)

The common foci activated during the PET and fMRI experiments were the bilateral middle frontal gyrus (BA 46), bilateral inferior frontal gyrus (BA 44/6), right middle frontal gyrus (BA 9/10), bilateral inferior parietal lobulus (BA 40), and left cingulate gyrus (BA 32). The additional activation foci revealed by fMRI included the left middle frontal gyrus (BA 9/10), right anterior cingulate gyrus (BA 32), right posterior cingulate gyrus (BA 23), left cuneus, and bilateral corpus callosum. The activation within the corpus callosum may reflect slight motion of the subject.

TABLE II. Numbers of PET and fMRI focal brain activations for each subject*

| Subject | 1.1 | 1.2 | 1.3 | 1.4 | 1.5 | 1.6 | Total |
|---|---|---|---|---|---|---|---|
| PET activations | 6 | 11 | 10 | 8 | 8 | 7 | 50 |
| fMRI activations | 11 | 14 | 16 | 15 | 18 | 8 | 82 |
| PET and fMRI | 6 | 11 | 10 | 7 | 8 | 4 | 46 |

\* For direct PET and fMRI comparison, only the PET activations located within the brain volume sampled by fMRI were reported.

**TABLE III. Comparison of PET and fMRI focal brain activations during verb generation for subject 1.1 (slice position: z = +18 mm above AC-PC line)***

| Structure | Brodmann area | fMRI activation | PET activation | | | |
|---|---|---|---|---|---|---|
| | | | Hemisphere | x | y | z |
| GFi | 44 | Lert | Left | −50 | 8 | 18 |
| | | Right | Right | 53 | 8 | 18 |
| | 45 | Left | Left | −47 | −18 | 18 |
| | | Left | Left | −32 | −5 | 18 |
| GTs | 22 | Left | Left | −48 | 45 | 18 |
| | | Right | | | | |
| Caudate | | Right | Right | 10 | 27 | 18 |
| | | Left | | | | |
| GOm | 19 | Left | | | | |
| | 18 | Left | | | | |
| | | Right | | | | |

* GFi, gyrus frontalis inferior; GFm, gyrus fontalis medium; GTs, gyrus temporalis superior; GOm, gyrus occipitalis mediums. PET activation location was reported in millimeters according to the AC-PC proportional grid system based on the atlas of Talairach and Tournoux [1988]. x, left-right with right hemisphere positive; y, anterior-posterior with anterior positive; z, superior-inferior with superior positive. Only the PET activations located within the brain volume sampled by fMRI are reported.

### Subject 1.4 (Table VI)

The PET activations included the left inferior frontal gyrus (BA 45), left superior temporal gyrus (BA 22), left middle temporal gyrus (BA 37), visual cortex (BAs 18 and 19), left corpus callosum (possible artifact), and left thalamus. The fMRI experiment successfully duplicated the PET activations except for the activation in the left corpus callosum, and detected more activation foci in the right middle frontal gyrus (BA 10), left insula, right superior temporal gyrus (BA 22), left middle temporal gyrus (BA 21), right thalamus, and basal ganglia.

**TABLE IV. Comparison of PET and fMRI focal brain activations during verb generation for subject 1.2 (z = −16 mm)***

| Structure | Brodmann area | fMRI activation | PET activation | | | |
|---|---|---|---|---|---|---|
| | | | Hemisphere | x | y | z |
| GFi | 47 | Left | Left | −37 | −27 | −16 |
| | | Left | Left | −23 | −21 | −16 |
| | | Right | Right | 46 | −26 | −16 |
| GTs | 38 | Right | Right | 40 | −2 | −16 |
| GTi/GF | 37 | Left | Left | −19 | 35 | −16 |
| | | Left | Left | −25 | 53 | −16 |
| | | Left | Left | −27 | 64 | −16 |
| | | Right | | | | |
| GTm | 21 | Left | | | | |
| Gh | 34 | Left | | | | |
| Brain stem | | Left | Left | −2 | 24 | −16 |
| Cerebellum | | Right | Right | 8 | 55 | −16 |
| | | Left | Left | −3 | 65 | −16 |
| Optic chiasm | | Center | Center | 0 | 0 | −16 |

* GFi, gyrus frontalis inferior; GTs, gyrus temporalis superior; GTi, gyrus temporalis; GF, gyrus fusiformis; GTm, gyrus temporalis medium; Gh, gyrus parahippocampi. Other conventions are the same as for Table III.

TABLE V. Comparison of PET and fMRI focal brain activations during verb generation for subject 1.3 (z = +24 mm)*

| Structure | Brodmann area | fMRI activation | PET activation | | | |
|---|---|---|---|---|---|---|
| | | | Hemisphere | x | y | z |
| GFm | 46 | Left | Left | −40 | −37 | 24 |
| | | Left | Left | −49 | −22 | 24 |
| | | Right | Right | 38 | −39 | 24 |
| GFi/GPrC | 44, 6 | Left | Left | −58 | −5 | 24 |
| | | Right | Right | 26 | −3 | 24 |
| GFm/GFs | 10, 9 | Right | Right | 19 | −46 | 24 |
| | | Left | | | | |
| LPi | 40 | Left | Left | −64 | 26 | 24 |
| | | Left | Left | −64 | 38 | 24 |
| | | Right | Right | 46 | 39 | 24 |
| GC | 32 | Left | Left | −8 | −32 | 24 |
| | | Right | | | | |
| | 23 | Right | | | | |
| Cuneus | 18 | Left | | | | |
| CC | | Left | | | | |
| | | Right | | | | |

* GFm, gyrus frontalis medius; GFi, gyrus frontalis inferior; GPrC, gyrus precentralis; GFs, gyrus frontalis superior; LPi, lobulus parietalis inferior; GC, gyrus cinguli; CC, corpus callosum. Other conventions are the same as for Table III.

TABLE VI. Comparison of PET and fMRI focal brain activations during verb generation for subject 1.4 (z = +4 mm)*

| Structure | Brodmann area | fMRI activation | PET activation | | | |
|---|---|---|---|---|---|---|
| | | | Hemisphere | x | y | z |
| GFi | 45 | Left | Left | −40 | −33 | 4 |
| GFm | 10 | Right | | | | |
| Insula | | Left | | | | |
| GTs | 22 | Left | Left | −49 | 25 | 4 |
| | | Left | Left | −63 | 29 | 4 |
| | | Right | | | | |
| GTm | 21 | Left | | | | |
| | 37 | Left | Left | −54 | 77 | 4 |
| GOm/Gh | 19 | Left | Left | −32 | 66 | 4 |
| | 18 | Right | Right | 20 | 79 | 4 |
| | 18 | Left | | | | |
| CC | | | Left | −18 | −28 | 4 |
| Basal ganglion | | Left | | | | |
| | | Right | | | | |
| Thalamus | | Left | Left | −10 | 17 | 4 |
| | | Right | | | | |

* GFi, gyrus frontalis inferior; GFm, gyrus frontalis medius; GTs, gyrus temporalis superior; GTm, gyrus temporalis medius; GOm, gyrus occipitalis medius; Gh, gyrus parahippocampi; CC, corpus callosum. Other conventions are the same as for Table III.

TABLE VII. Comparison of PET and fMRI focal brain activations during verb
generation for subject 1.5 (z = +4 mm)*

| Structure | Brodmann area | fMRI activation | PET activation | | | |
|---|---|---|---|---|---|---|
| | | | Hemisphere | x | y | z |
| GFi | 46 | Left | Left | −49 | −32 | 4 |
| | 46 | Right | | | | |
| | 45 | Left | Left | −51 | −17 | 4 |
| | 45 | Right | | | | |
| Insula | | Left | Left | −37 | −17 | 4 |
| | | Right | | | | |
| GTs | 22 | Left | Left | −60 | 12 | 4 |
| | | Right | | | | |
| GTm | 21 | Left | | | | |
| | | Right | Right | 46 | 39 | 4 |
| GOm/Gh | 18 | Left | Left | −23 | 88 | 4 |
| | | Right | Right | 28 | 85 | 4 |
| | | Left | Left | −1 | 53 | 4 |
| | 19 | Right | | | | |
| Thalamus | | Left | | | | |
| | | Right | | | | |
| Basal ganglion | | Left | | | | |
| | | Right | | | | |

* GFi, gyrus frontalis inferior; GTs, gyrus temporalis superior; GTm, gyrus temporalis medius; GOm, gyrus occipitalis medius; Gh, gyrus parahippocampi. Other conventions are the same as for Table III.

## Subject 1.5 (Table VII)

Significant signal changes were observed in the left inferior frontal cortex (BAs 45 and 46), left insula, left superior temporal gyrus (BA 22), right middle temporal gyrus (BA 21), and bilateral middle occipital gyrus (BA 18) for both the PET and fMRI experiments. In addition to the activation foci detected by both PET and fMRI, the right inferior frontal cortex (BAs 45 and 46), right insula, right superior temporal gyrus (BA 22),

TABLE VIII. Comparison of PET and fMRI focal brain activations during verb
generation for subject 1.6 (z = +20 mm)*

| Structure | Brodmann area | fMRI activation | PET activation | | | |
|---|---|---|---|---|---|---|
| | | | Hemisphere | x | y | z |
| GC | 24 | | Right | 4 | −21 | 20 |
| GFi | 45 | Left | Left | −23 | −21 | 20 |
| | | | Right | 40 | −26 | 20 |
| GPrC | 6 | Left | | | | |
| | | | Right | 50 | −4 | 20 |
| | 4 | Left | Left | −47 | 10 | 20 |
| | | Right | Right | 53 | 11 | 20 |
| GTs | 22 | Left | | | | |
| | | Right | | | | |
| GOm | 19 | Right | Right | 29 | 87 | 20 |
| FOF | | Right | | | | |

* GFd, gyrus frontalis medialis; GC, gyrus cinguli; GFi, gyrus frontalis inferior; GPrC, gyrus precentralis; GTs, gyrus temporalis superior; GOm, gyrus occipitalis medius; FOF, fasciculus occipito-frontalis. Other conventions are the same as for Table III.
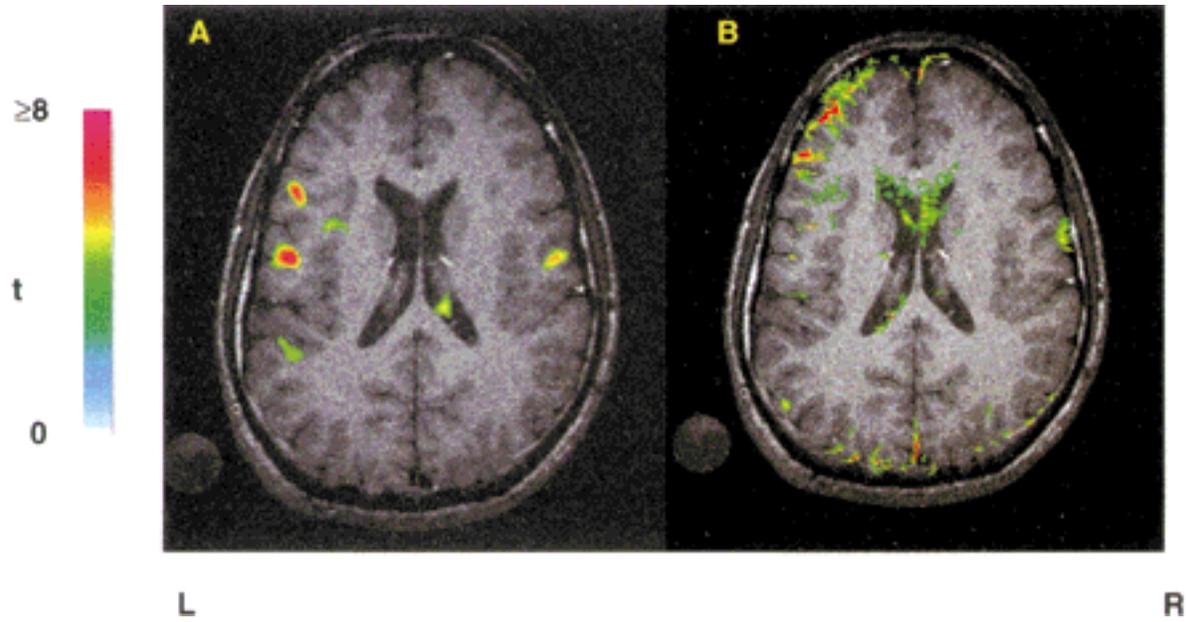
**Figure 2.**
Representative PET and fMRI activations for language for an individual subject (subject 1.1). **A:** PET activation image. **B:** fMRI activation image. The PET activation image has been transformed into stereotactic space. Center of the image plane is 18 mm above AC-PC line. Color scale represents t value of each pixel. R, right hemisphere; L, left hemisphere.
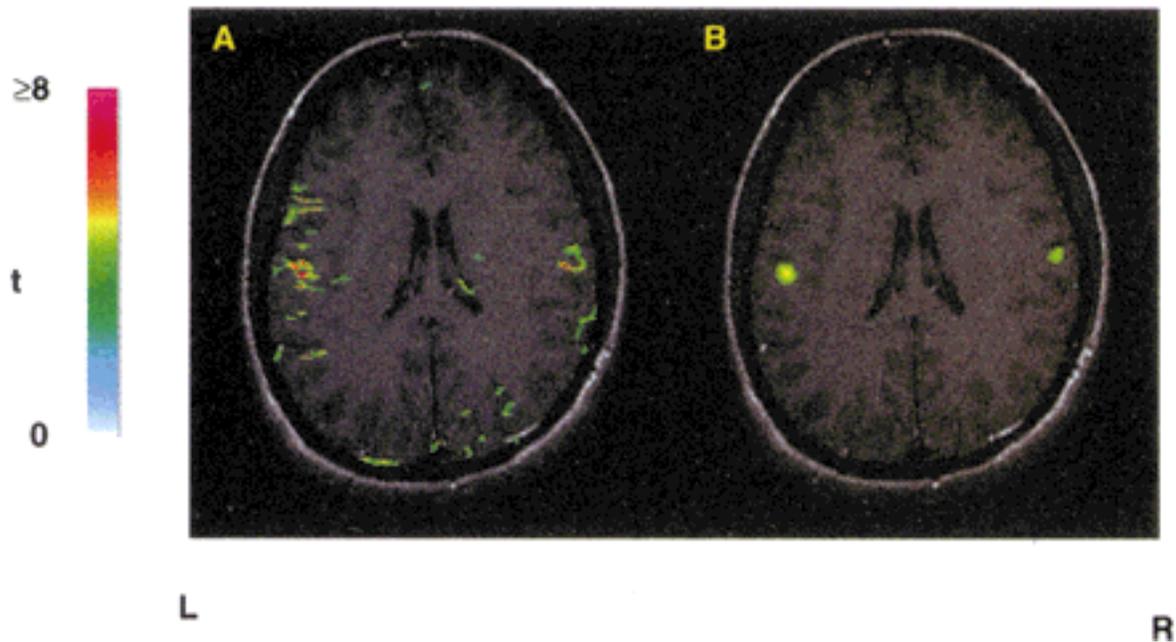


**Figure 3**.
Functional MRI activations for language for an individual subject (subject 1.6). **A:** High-resolution fMRI. **B:** Low-resolution fMRI. The low-resolution fMRI was obtained by spatially smoothing raw fMRI data to 8 mm FWHM to match PET resolution, thereby illustrating the effect of spatial resolution on detection of activations. Center of the image plane is 20.2 mm above AC-PC line. Color scale represents t value of each pixel. R, right hemisphere; L, left hemisphere.

left middle temporal gyrus (BA 21), right middle occipital gyrus (BA 19), thalamus, and basal ganglia were also activated in the fMRI experiment.

### Subject 1.6 (Table VIII)

Significant signal changes for both PET and fMRI included the left inferior frontal gyrus (BA 45), bilateral precentral gyrus (BA 4), and right middle occipital gyrus (BA 19). Three activation foci, the right inferior frontal gyrus (BA 45), right cingulate gyrus (BA 24), and right precentral gyrus (BA 6), were detected by PET only. The other four activation foci, the left middle occipital gyrus (BA 18), left precentral gyrus (BA 6), bilateral superior temporal gyrus (BA 22), and right occipital-frontal fasciculus, were only seen in the fMRI experiment. The fMRI result for this subject disagreed with the PET findings, in which the whole-brain PET data indicated right-hemispheric dominance and the limited brain volume PET showed no lateralization effect, but the fMRI indicated left-hemispheric dominance.

The significant activations for high-resolution and low-resolution fMRI for this subject are shown in Figure 3. Figure 3A is high-resolution fMRI (1.4 mm FWHM), and Figure 3B is low-resolution fMRI (8 mm FWHM). The significant level is the same for both high- and low-resolution fMRI. The low-resolution fMRI image was obtained by spatially smoothing the raw fMRI data to 8 mm FWHM to match the PET spatial resolution. The same intensity (t = 3.7) and extent (K = 14) thresholds used for the PET data analysis were used to analyze the low-resolution fMRI images. Figure 3 shows that the number of activations detected in low-resolution fMRI is much lower than in high-resolution fMRI and demonstrates that high-resolution imaging is more sensitive in detecting neural activity.

### fMRI-only study

The intensity-weighted areas of significant activations in the selected ROIs, which include BAs 22 and 44–46 (BA 47 was not covered by the selected fMRI slice) for the 9 volunteers (group 2), are shown in Figure 4. Pronounced activations were observed in the left inferior frontal gyrus (BAs 44 and 45) and the left superior temporal gyrus (BA 22). A repeated-measure analysis of variance (ANOVA) with a X b
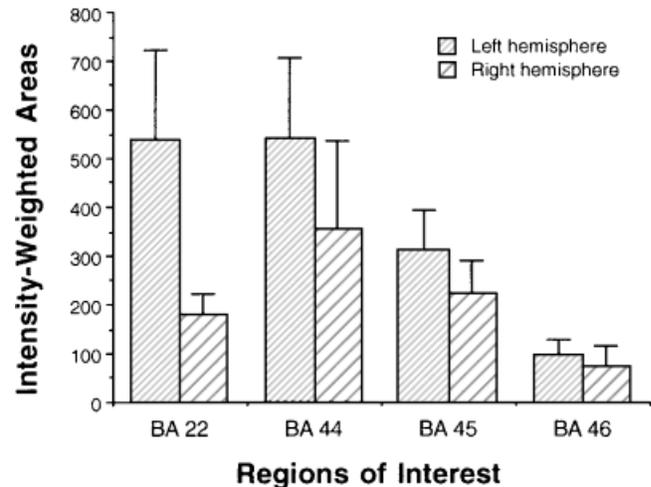


**Figure 4.**
Intensity-weighted areas of significant activations in the selected regions of interest, which include BAs 22 and 44–46 for the 9 volunteers (BA 47 was not covered by the selected fMRI slice). Error bars represent one standard error.

factorial design, with structure (i.e., ROI) and hemisphere as factors and the normalized intensity-weighted areas of activations as the dependent measure, revealed significant effects of structure (F(3,64) = 6.2, $P < 0.01$) and hemisphere (F(1,64) = 10.8, $P < 0.01$). The intensity-weighted areas of activations in the left hemisphere were significantly larger than those in the right hemisphere ($P < 0.01$, ANOVA). This demonstrates that, when considering the 9 subjects as a group, the left hemisphere is clearly dominant for language.

Figure 5 presents the average activation map for group 2 subjects for verb generation. Significant activations were predominantly found in the left inferior frontal gyrus (BAs 44 and 45) and superior temporal gyrus (BA 22). The homologous right-hemisphere regions showed much smaller areas of activation. This clearly demonstrates that, for the majority of subjects, the left hemisphere is involved to a greater extent in language processing than is the right hemisphere.

The lateralization index for each individual is summarized in Table IX for group 2 subjects. The values of the lateralization index ranged from −0.45–+0.79. Table IX shows that 7 out of 9 subjects exhibited left-hemispheric dominance and 2 out of 9 (subject 2.1 [female, right-handed] and subject 2.6 [male, right-handed]) exhibited right-hemispheric dominance.

Representative functional activations for language for individual subjects are illustrated in Figure 6.-
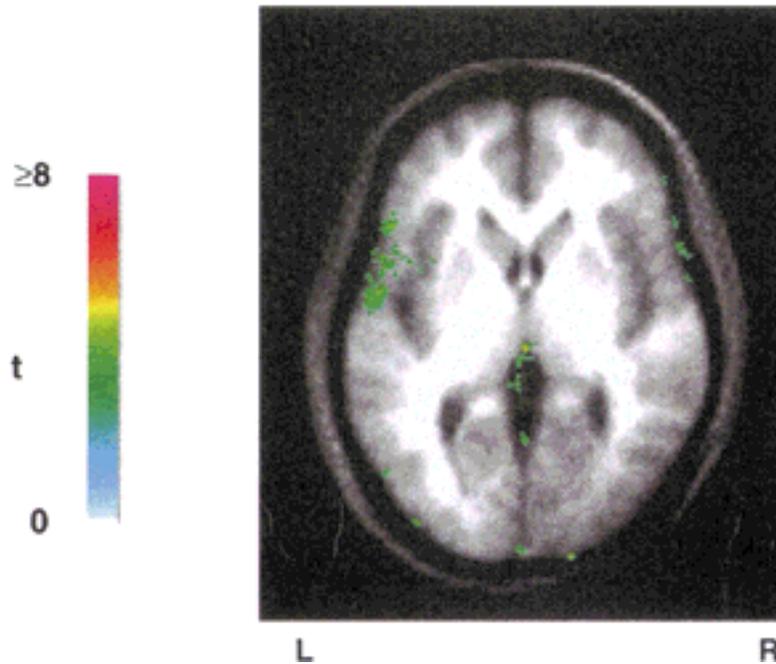
**Figure 5.**
Average brain activations involved in verb generation task detected using fMRI (group 2). Activation information has been transformed into stereotactic space and averaged across the 9 subjects in group 2. Center of the image plane is 4 mm above AC-PC line. Color scale represents t value of each pixel. R, right hemisphere; L, left hemisphere.
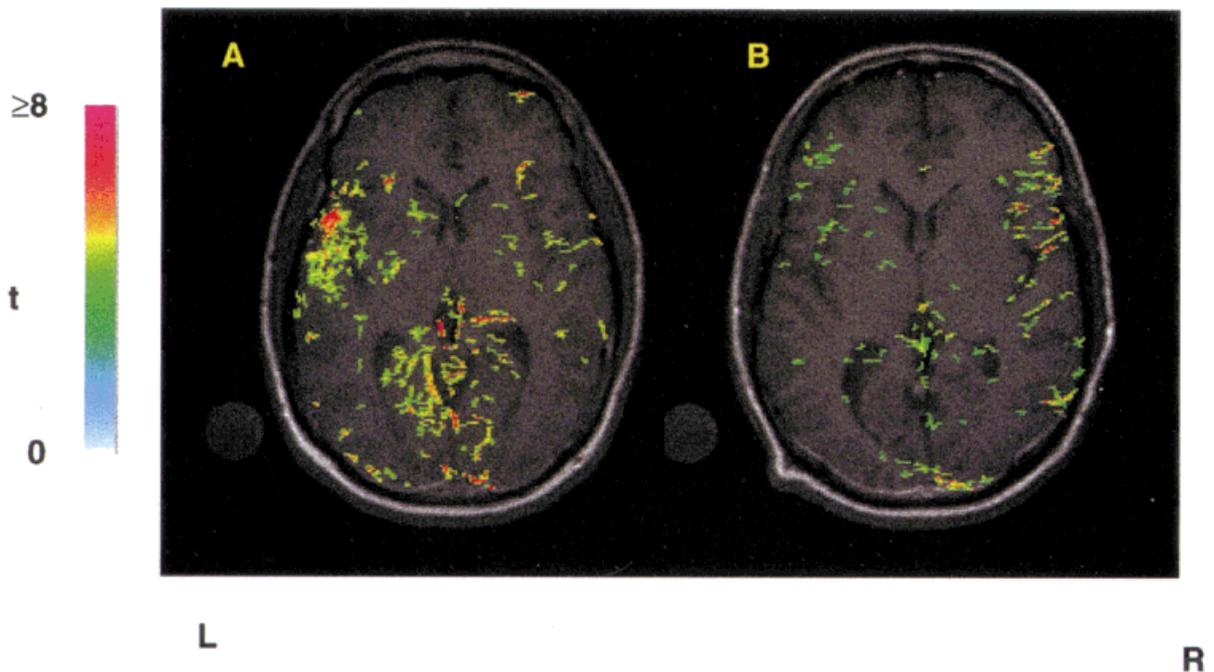


**Figure 6.**
Representative fMRI activations for language for individual subjects. **A:** Example of left-hemispheric dominance (subject 2.2). **B:** Example of right-hemispheric dominance (subject 2.1). Center of the image plane is 4 mm above AC-PC line. Color scale represents t value of each pixel. R, right hemisphere; L, left hemisphere.

TABLE IX. Functional MRI assessment of hemisphereic dominance for language*

| Subject | 2.1 | 2.2 | 2.3 | 2.4 | 2.5 | 2.6 | 2.7 | 2.8 | 2.9 |
|---|---|---|---|---|---|---|---|---|---|
| Gender | Female | Male | Female | Female | Female | Male | Male | Male | Male |
| Handiness | Right | Right | Right | Right | Right | Right | Right | Left | Right |
| LI | −0.13 | 0.47 | 0.41 | 0.60 | 0.14 | −0.45 | 0.49 | 0.57 | 0.79 |
| Laterality | Right | Left | Left | Left | Left | Right | Left | Left | Left |

* LI, Lateralization index computed using the intensity-weighted area of BAs 22 and 44–47.

Figure 6A is an example of left-hemispheric dominance, and Figure 6B is an example of right-hemispheric dominance. The activation of these individual subjects reflects individual variability not seen on the group analysis average. In Figure 6A (subject 2.2), significant activation was predominantly found in the left inferior frontal gyrus (primarily BAs 44 and 45) and left superior temporal gyrus (BA 22). The homologous right-hemisphere regions showed a much weaker activation with a much smaller extent. Bilateral activations were found in the basal ganglia and lingual gyrus (BAs 18 and 19). Right-hemisphere activation was also seen in the middle frontal gyrus (BA 10). In Figure 6B (subject 2.6), significant activation was observed in the superior temporal gyrus (BA 22) and bilateral lingual gyrus (BAs 18 and 19). Bilateral activations were also seen in BA 44 (inferior frontal gyrus). A large activation area was shown in the right inferior frontal gyrus within BAs 45 and 46; little or no activation was seen in the homologous regions of the left inferior frontal gyrus. The right basal ganglion, left thalamus, and both left and right cuneus (BA 18) were also activated significantly.

## DISCUSSION AND CONCLUSIONS

This study suggests that the fMRI technique, even using a conventional (nonecho-planar) MRI scanner, can be useful in evaluating hemispheric dominance for language. By group analysis, our PET/fMRI and fMRI-only studies were in concordance with previous PET results and showed left-hemispheric dominance for language [Petersen et al., 1988, 1989; Wise et al., 1991]. However, for individual subjects, the dominant hemisphere did show some variability, with 7 out of 9 subjects having left-hemispheric dominance and 2 subjects having right-hemispheric dominance for both groups 1 and 2. A direct comparison between PET and fMRI demonstrated that fMRI can successfully replicate PET findings. About 92% of the activation foci detected by PET were detected by fMRI. On the other hand, fMRI reported 64% more activations than PET did.

Several factors may account for the greater amount of activation detected by fMRI. First, PET has a much lower spatial resolution than does fMRI (8 mm vs. 1.4 mm for this study) and is likely to miss highly focal activations, as illustrated in Figure 3. Second, the differences in the physiological processes associated with the neural activity of the brain revealed by PET and fMRI may also contribute to the discrepancy in the number of activations. Using $^{15}$O, PET measures rCBF as an increase in flux of labeled water into brain tissue. Using the BOLD technique, fMRI measures local hyperoxia in capillaries and veins. Local hyperoxia (seen by fMRI) is caused by a local increase in rCBF, which also causes the increase in plasma flux seen by PET. That is, PET and fMRI detect different biophysical effects of a single cause (increase in rCBF). Yet, the extent to which the fMRI BOLD technique spatially correlates with the rCBF change detected with PET is still unclear. Third, PET data were acquired with an interslice distance of 6.5 mm. For the PET/fMRI comparison, the PET data were resliced using linear interpolation to a 10-mm slice thickness, to match the fMRI data. Interpolation to a slice, rather than direct acquisition from that slice, may cause PET to miss some activations. Fourth, the sensitivity of fMRI is different from that of PET. It is well-known that the signal change of PET during neural activity is higher than that of fMRI. The magnitude of PET rCBF signal change can be up to 50% for simple visual stimulation [Fox and Raichle, 1984; Fox et al., 1986] and 5% for cognitive tasks [Wise et al., 1991; Paulesu et al., 1995]. The typical signal change for fMRI seems to be about 2–4% during cognitive tasks [Cohen et al., 1994] at a 1.5-T magnet field strength. However, due to the fact that many more images are typically acquired for fMRI than for PET in a single session (e.g., 112 vs. 6 images, in the present study), fMRI may be more sensitive than PET on this basis. Finally, the interpretation of fMRI data may also be confounded by the possible presentation of artifactual

signal changes, which could result from head motion [Hajnal et al., 1994], inflow effect [Duyn et al., 1994; Kim et al., 1994], and nonspecific processes such as veins draining from the sites of neural activity [Lai et al., 1993]. Given the fact that fMRI signal change is only a few percentages of the original MRI image, even subvoxel head motion could result in much larger artifactual signal than the real fMRI signal, especially in areas with abrupt signal change relative to their neighbors (for example, at a brain boundary). In contrast, PET rCBF signal change is much larger and the spatial resolution is lower than with fMRI. These factors enable PET to tolerate much more patient motion effect than fMRI. Future studies are necessary to address in greater detail whether the above issues account for the discrepancy between the present PET and fMRI findings for language.

Our individual subject-by-subject PET analysis (group 1 subjects) revealed that 7 out of the 9 subjects exhibited left-hemispheric dominance for language and that 2 out of the 9 subjects exhibited right-hemispheric dominance. The fMRI results showed that the same percentage of group 2 subjects were right-hemisphere dominant. Previous patient studies using the Wada test have shown that 4–20% of right-handed subjects can have a right-hemispheric dominance for language [Rasmussen and Milner, 1977; Pardo and Fox, 1993; Binder et al., 1995; Desmond et al., 1995]. Previous PET single-subject analysis also indicated that 11% of right-handed subjects (1 out of 9) have a right-hemispheric dominance for language [Pardo and Fox, 1993]. Thus, our observations on the population distribution of hemispheric dominance for language are in agreement with previous results of PET and the Wada test.

Despite being consistent with a previous PET study with patients [Pardo and Fox, 1993], PET studies with normal volunteers [Petersen et al., 1988, 1989; Wise et al., 1991], and fMRI studies with patients [Binder et al., 1995; Desmond et al., 1995], our results were contradictory with previous cognitive fMRI studies with normal healthy volunteers. More specifically, Shaywitz et al. [1995a] and Cohen et al. [1993, 1994] showed no hemispheric asymmetry of activation for language and memory. One reason for the conflicting findings may be the different procedures used for determining lateralization. The studies of Shaywitz et al. [1995a] and Cohen et al. [1993, 1994] detected brain activations based on individual subject-by-subject analysis. Hemispheric lateralization was determined for the group of subjects using an ANOVA statistical analysis, with hemisphere and brain structure as the factors and number of activations as the dependent measure. In

the present study, lateralization was determined for both individual subjects and for the group of subjects. In the group analysis, a similar ANOVA analysis procedure was applied, except that the normalized intensity-weighted areas of activations were used as the dependent measure instead of the number of activations. The number of activations may be not a good indicator of the brain's participation in a particular task performance because information about the intensity and spatial extent of the activation foci is ignored. The intensity-weighted area of activations, used in the present study to assess the lateralization of activation, is a single parameter that includes the combined effects of intensity, spatial extent, and number of activations. Similar strategies have also been used by Binder et al. [1995] and Desmond et al. [1995] to assess the dominant hemisphere for language for epileptic patients, and have demonstrated the possibility of using fMRI as an alternative to the Wada test in clinical practice.

The major limitation for our fMRI study is the use of the single-slice sampling technique. With only a small portion of the brain being sampled, we are missing some brain areas that participate in language perception and production, which may result in possible mislateralization. Even if one targets a particular brain region (for example, the inferior frontal gyrus), the single-slice sampling technique is still not sufficient. This is because of the difficulty in predicting the exact locations of the brain regions that are likely to activate for language for individual subjects, due to intersubject anatomical variability in cortical functional organization. It has been shown by Fox and Pardo [1991] that intersubject anatomical variability is about 4–8 mm for primary and associated cortices. With a slice thickness of 5–10 mm, which is commonly used in fMRI experiments, the targeted activation foci could be missed. Thus, we believe that future fMRI studies should be pursued using the multiple-slice or 3D acquisition technique.

In summary, the results of this study indicate that it is possible to use the conventional fMRI technique to evaluate hemispheric dominance for language. Group analysis (averaged across subjects) showed left-hemispheric dominance for language and is in concordance with previous PET results. Individual subject-by-subject analysis revealed that the dominant hemisphere shows some variability, with 7 out of 9 subjects having left-hemispheric dominance and 2 subjects having right-hemispheric dominance. The direct comparison between PET and fMRI further demonstrated that the fMRI technique can replicate PET findings, in that 92% of the activation foci detected by PET were also found

by fMRI. This study suggests that fMRI might be useful in clinical practice as an alternative to the invasive Wada test to evaluate the dominant hemisphere for language. Future research will focus on direct clinical trials and patient studies, using the multiple-slice fMRI technique.

## ACKNOWLEDGMENTS

## REFERENCES

Bandettini PA, Wong EC, Hinks RS, Tikodsky RS, Hyde JS (1992): Time course EPI of human brain function during task activation. Magn Reson Med 25:390–397.

Bandettini PA, Jesmanowicz A, Wong EC, Hyde JS (1993a): Processing strategies for time-course data sets in functional MRI of the human brain. Magn Reson Med 30:161–173.

Bandettini PA, Wong EC, DeYoe EA, Binder JR, Rao SM, Birzer D, Estkowski LD, Jesmanowicz A, Hinks RS, Hyde JS (1993b): The functional dynamics of blood oxygen level dependent contrast in the motor cortex. Proc Soc Magn Reson Med 1382.

Binder JR, Swanson SJ, Hammeke TA, Morris GL, Mueller WM, Fischer M, Frost JA, Rao SM (1995): Determination of language dominance with functional MRI: A comparison with the Wada test. Hum Brain Mapping 1:235.

Cohen JD, Forman SD, Casey BJ, Noll DC (1993): Spiral-scan imaging of dorsolateral prefrontal cortex during a working memory task. Proc Soc Magn Reson Med 330.

Cohen JD, Forman SD, Braver TS, Casey BJ, Servan-Schreiber D, Noll DC (1994): Activation of the prefrontal cortex in a nonspatial working memory task with functional MRI. Hum Brain Mapping 1:293–304.

Constable RT, McCarthy G, Allison T, Anderson SW, Gore JC (1993): Functional brain imaging at 1.5 T using conventional gradient echo MR imaging techniques. Magn Reson Imaging 11:451–459.

Desmond J, Sum JM, Wagner AD, Demb JB, Shear PK, Glover GH, Gabrieli JD, Morrell MJ (1995): Language lateralization in epileptic patients: A clinical application for functional MRI. In: FMRI Workshop: How to Interpret It, How to Do It, San Francisco, pp 54–63.

Duyn JH, Moonen CTW, VanYperen GH, DeBoer RW, Luyten PR (1994): Inflow versus deoxyhemoglobin effects in BOLD functional MRI using gradient echoes at 1.5 T. Nucl Magn Reson Biomed 7:83–88.

Fox PT, Pardo JV (1991): Does inter-subject variability in cortical functional organization increase with neural ''distance'' from the periphery? Ciba Found Symp 163:125–144.

Fox PT, Raichle ME (1984): Stimulus rate dependence of regional cerebral blood flow in human striate cortex, demonstrated by positron emission tomography. J Neurophysiol 51:1109–1120.

Fox PT, Perlmutter JS, Raichle ME (1985): A stereotactic method of anatomical localization for positron emission tomography. J Comput Assist Tomogr 9:141–153.

Fox PT, Mintun MA, Raichle ME, Miezin FM, Allman JM, Van Essen DC (1986): Mapping human visual cortex with positron emission tomography. Nature 323:806–809.

Fox PT, Mintun MA, Reiman EM, Raichle ME (1988): Enhanced detection of focal brain responses using intersubject averaging and change-distribution analysis of subtracted PET images. J Cereb Blood Flow Metab 8:642–653.

Francis WN, Kucera H (1982): Frequency Analysis of English Usage: Lexicon and Grammar, Boston: Houghton Mifflin Co.

Hajnal JV, Myers R, Oatridge A, Schwieso JE, Young IR, Bydder GM (1994): Artifacts due to stimulus correlated motion in functional imaging of the brain. Magn Reson Med 31:283–291.

Hertz-Pannier L, Gaillard WD, Mott S, Cuenod CA, Bookheimer S, Weinstein S, Conry J, Theodore WH, LeBihan D (1994): Preoperative assessment of language lateralization by fMRI in children with complex partial seizures: Preliminary study. Proc Soc Magn Reson Med 326.

Kim SG, Ashe J, Hendrich K, Ellermann JM, Merkle H, Ugurbil K, Georgopolis AP (1993): Functional magnetic resonance imaging of motor cortex: Hemispheric asymmetry and handedness. Science 261:613–617.

Kim SG, Hendrich K, Hu X, Merkle H, Ugurbil K (1994): Potential pitfalls of functional MRI using conventional gradient-recalled echo techniques. Nucl Magn Reson Biomed 7:69–74.

Kwong KK, Belliveau JW, Chesler DA, Goldberg IE, Weisskoff RM, Poncelet BP, Kennedy DN, Hoppel BE, Cohen MS, Turner R, Cheng HM, Brady TJ, Rosen BR (1992): Dynamic magnetic resonance imaging of human brain activity during primary sensory stimulation. Proc Natl Acad Sci USA 89:5675–5679.

Lai S, Hopkins AL, Haacke EM, Li D, Wasserman BA, Buckley P, Friedman L, Meltzer H, Hedera P, Friedland R (1993): Identification of vascular structures as a major source of signal contrast in high resolution 2D and 3D functional activation imaging of the motor cortex at 1.5 T: Preliminary results. Magn Reson Med 30:387–392.

Lancaster JL, Glass TG, Lankipalli BR, Downs H, Mayberg H, Fox PT (1995): A modality-independent approach to spatial normalization of tomographic images of the human brain. Hum Brain Mapping 3:209–223.

McCarthy G, Blamire AM, Rothman DL, Gruetter R, Shulman RG (1993): Echo-planar magnetic resonance imaging studies of frontal cortex activation during word generation in humans. Proc Natl Acad Sci USA 90:4952–4956.

Menon RS, Ogawa S, Kim SG, Ellermann JM, Merkle H, Tank DW, Ugurbil K (1992): Functional brain mapping using magnetic resonance imaging: Signal change accompanying visual stimulation. Invest Radiol 27:47–53.

Mintun MA, Fox PT, Raichle ME (1989): A highly accurate method of localizing regions of neuronal activation in the human brain with positron emission tomography. J Cereb Blood Flow Metab 9:96–103.

Ogawa S, Tank DW, Menon R, Ellermann JM, Kim SG, Merkle H, Ugurbil K (1992): Intrinsic signal changes accompanying sensory stimulation: Functional brain mapping with magnetic resonance imaging. Proc Natl Acad Sci USA 89:5951–5955.

Paivio A, Yuille JC, Madigan SA (1968): Concreteness, imagery, and meaningfulness values for 925 nouns. J Exp Psychol Monogr [Suppl] 76:1–25.

Pardo JV, Fox PT (1993): Preoperative assessment of the cerebral hemispheric dominance for language with CBF PET. Hum Brain Mapping 1:57–68.

Paulesu E, Frith CD, Frackowiak RSJ (1993): The neural correlates of the verbal component of working memory. Nature 362:342–345.

Paulesu E, Connelly A, Frith CD, Friston KJ, Healther J, Myers R, Gadian DG, Frackowiak RSJ (1995): Functional MR imaging correlations with positron emission tomography: Initial experience using cognitive activation paradigm on verbal working memory. Funct Neuroimaging 5:207–225.

Petersen SE, Fox PT, Posner MI, Mintun M, Raichle ME (1988): Positron emission tomographic studies of the cortical anatomy of single-word processing. Nature 331:585–589.

Petersen SE, Fox PT, Posner MI, Mintun M, Raichle ME (1989): Positron emission tomographic studies of the processing of single words. J Cogn Neurosci 1:153–170.

Raichle ME, Fiez JA, Videen TO, MacLeod AM, Pardo JV, Fox PT, Petersen SE (1994): Practice-related changes in human brain functional anatomy during nonmotor learning. Cereb Cortex 4:8–26.

Rao SM, Binder JR, Bandettini PA, Hammeke TA, Yetkin FZ, Jesmanowicz A, Lisk LM, Morris GL, Mueller WM, Estkowski LD, Wong EC, Haughton VM, Hyde JS (1993): Functional magnetic resonance imaging of complex human movements. Neurology 43:2311–2318.

Rasmussen T, Milner B (1977): The role of early left-brain injury in determining lateralization of cerebral speech functions. Ann NY Acad Sci 299:355–369.

Schad LR, Wenz F, Knopp MV, Baudendistel K, Muller E, Lorenz WJ (1994): Functional 2D and 3D magnetic resonance imaging of motor cortex stimulation at high spatial resolution using standard 1.5 T imager. Magn Reson Imaging 12:9–15.

Schneider W, Noll DC, Cohen JD (1993): Functional topographic mapping of the cortical ribbon in human vision with conventional MRI scanners. Nature 365:150–152.

Sergent J, Zuck E, Levesque M, MacDonald B (1992): Positron emission tomography study of letter and object processing: Empirical finding and methodological considerations. Cereb Cortex 80:68–80.

Shallice T, Fletcher P, Frith CD, Grasby P, Frackowiak RS, Dolan RJ (1994): Brain regions associated with acquisition and retrieval of verbal episodic memory. Nature 368:633–635.

Shaywitz BA, Kenneth R, Pugh KR, Constable RT, Shaywitz SE, Bronen RA, Fulbright RK, Shankweiler DP, Katz L, Fletcher JM, Skudlarski P, Gore JC (1995a): Localization of semantic processing using functional magnetic resonance imaging. Hum Brain Mapping 2:149–158.

Shaywitz BA, Shaywitz SE, Pugh KR, Constable RT, Skudlarski P, Fulbright RK, Bronen RA, Fletcher JM, Shankweiler DP, Katz L, Gore JC (1995b): Sex differences in the functional organization of the brain for language. Nature 373:607–609.

Talairach J, Tournoux P (1988): Co-Planar Stereotaxic Atlas of the Human Brain. Three-Dimensional Proportional System: An Approach to Cerebral Imaging, New York: Thieme Medical Publishers, Inc.

Wada JA (1949): A new method for the determination of the side of cerebral speech dominance. A preliminary report on the intracarotid injection of sodium amytal in man. Igaku to Seibutsugaku 14:221–222 (in Japanese).

Wada J, Rasmussen T (1960): Intracarotid injection of sodium amytal for the lateraliztaion of cerebral speech dominance. J Neurosurg 17:266–282.

Wise R, Chollet F, Hadar U, Friston K, Hoffner E, Frackowiak R (1991): Distribution of cortical neural networks involved in word comprehension and word retrieval. Brain 114:1803–1817.

Woods RP, Mazziotta JC, Cherry SR (1993): MRI-PET registration with automated algorithm. J Comput Assist Tomogr 17:536–546.

Xiong J, Gao JH, Lancaster JL, Fox PT (1995): Clustered pixels analysis for functional MRI activation studies of the human brain. Hum Brain Mapping 3:287–301.